IRis

Northeastern University

Physics Faculty Publications

Department of Physics

July 01, 2001

Spectra of "real-world" graphs: beyond the semicircle law

Illés J. Farkas
Eötvös University

Imre Derényi
Collegium Budapest and Institut Curie

Albert-László Barabási
Collegium Budapest and University of Notre Dame

Tamás Vicsek
Eötvös University and Collegium Budapest

Recommended Citation

Farkas, Illés J.; Derényi, Imre; Barabási, Albert-László; and Vicsek, Tamás, "Spectra of "real-world" graphs: beyond the semicircle law" (2001). *Physics Faculty Publications*. Paper 119. http://hdl.handle.net/2047/d20000692

This work is available open access, hosted by Northeastern University.

Spectra of "real-world" graphs: Beyond the semicircle law

Illés J. Farkas,[1,*] Imre Derényi,[2,3,†] Albert-László Barabási,[2,4,‡] and Tamás Vicsek[1,2,§]
[1]*Department of Biological Physics, Eötvös University, Pázmány Péter Sétány 1A, H-1117 Budapest, Hungary*
[2]*Collegium Budapest, Institute for Advanced Study, Szentháromság utca 2, H-1014 Budapest, Hungary*
[3]*Institut Curie, UMR 168, 26 rue d'Ulm, F-75248 Paris 05, France*
[4]*Department of Physics, University of Notre Dame, Notre Dame, Indiana 46556*
(Received 19 February 2001; published 20 July 2001)

Many natural and social systems develop complex networks that are usually modeled as random graphs. The eigenvalue spectrum of these graphs provides information about their structural properties. While the semicircle law is known to describe the spectral densities of uncorrelated random graphs, much less is known about the spectra of real-world graphs, describing such complex systems as the Internet, metabolic pathways, networks of power stations, scientific collaborations, or movie actors, which are inherently correlated and usually very sparse. An important limitation in addressing the spectra of these systems is that the numerical determination of the spectra for systems with more than a few thousand nodes is prohibitively time and memory consuming. Making use of recent advances in algorithms for spectral characterization, here we develop methods to determine the eigenvalues of networks comparable in size to real systems, obtaining several surprising results on the spectra of adjacency matrices corresponding to models of real-world graphs. We find that when the number of links grows as the number of nodes, the spectral density of uncorrelated random matrices does not converge to the semicircle law. Furthermore, the spectra of real-world graphs have specific features, depending on the details of the corresponding models. In particular, scale-free graphs develop a trianglelike spectral density with a power-law tail, while small-world graphs have a complex spectral density consisting of several sharp peaks. These and further results indicate that the spectra of correlated graphs represent a practical tool for graph classification and can provide useful insight into the relevant structural properties of real networks.

DOI: 10.1103/PhysRevE.64.026704 PACS number(s): 02.60.−x, 68.55.−a, 68.65.−k, 05.45.−a

I. INTRODUCTION

Random graphs [1,2] have long been used for modeling the evolution and topology of systems made up of large assemblies of similar units. The uncorrelated random graph model—which assumes each pair of the graph's vertices to be connected with equal and independent probabilities—treats a network as an assembly of equivalent units. This model, introduced by the mathematicians Paul Erdős and Alfréd Rényi [1], has been much investigated in the mathematical literature [2]. However, the increasing availability of large maps of real-life networks has indicated that real networks are fundamentally correlated systems, and in many respects their topology deviates from the uncorrelated random graph model. Consequently, the attention has shifted towards more advanced graph models which are designed to generate topologies in line with the existing empirical results [3–14]. Examples of real networks, that serve as a benchmark for the current modeling efforts, include the Internet [6,15–17], the World-Wide Web [8,18], networks of collaborating movie actors and those of collaborating scientists [13,14], the power grid [4,5], and the metabolic network of numerous living organisms [9,19].

These are the systems that we will call *"real-world" networks* or *graphs*. Several converging reasons explain the enhanced current interest in such real graphs. First, the amount of topological data available on such large structures has increased dramatically during the past few years thanks to the computerization of data collection in various fields, from sociology to biology. Second, the hitherto unseen speed of growth of some of these complex networks—e.g., the Internet—and their pervasiveness in affecting many aspects of our lives has created the need to understand the topology, origin, and evolution of such structures. Finally, the increased computational power available on almost every desktop has allowed us to study such systems in unprecedented detail.

The proliferation of data has lead to a flurry of activity towards understanding the general properties of real networks. These efforts have resulted in the introduction of two classes of models, commonly called *small-world graphs* [4,5] and the *scale-free networks* [10,11]. The first aims to capture the clustering observed in real graphs, while the second reproduces the power-law degree distribution present in many real networks. However, until now, most analyses of these models and data sets have been confined to real-space characteristics, which capture their static structural properties e.g., degree sequences, shortest connecting paths, and clustering coefficients. In contrast, there is extensive literature demonstrating that the properties of graphs and the associated adjacency matrices are well characterized by spectral methods, that provide global measures of the network properties [20,21]. In this paper we offer a detailed analysis of the

*Email address: fij@elte.hu
†Email address: derenyi@angel.elte.hu
‡Email address: alb@nd.edu
§Email address: vicsek@angel.elte.hu

 ©2001 The American Physical Society

most studied network models using algebraic tools intrinsic to large random graphs.

The paper is organized as follows. Section II introduces the main random graph models used for the topological description of large assemblies of connected units. Section III lists the—analytical and numerical—tools that we used and developed to convert the topological features of graphs into algebraic invariants. Section IV contains our results concerning the spectra and special eigenvalues of the three main types of random graph models: sparse uncorrelated random graphs in Sec. IV A, small-world graphs in Sec. IV B, and scale-free networks in Sec. IV C. Section IV D gives simple algorithms for testing the graph's structure, and Sec. IV E investigates the variance of structure within single random graph models.

II. MODELS OF RANDOM GRAPHS

A. The uncorrelated random graph model and the semicircle law

1. Definitions

Throughout this paper we will use the term ''*graph*'' for a set of points (vertices) connected by undirected lines (edges); no multiple edges and no loops connecting a vertex to itself are allowed. We will call two vertices of the graph ''*neighbors*,'' if they are connected by an edge. Based on Ref. [1], we shall use the term ''*uncorrelated random graph*'' for a graph if (i) the probability for any pair of the graph's vertices being connected is the same, p; (ii) these probabilities are independent variables.

Any graph G can be represented by its *adjacency matrix* $A(G)$, which is a real symmetric matrix: $A_{ij}=A_{ji}=1$, if vertices i and j are connected, or 0, if these two vertices are not connected. The main algebraic tool that we will use for the analysis of graphs will be the spectrum—i.e., the set of eigenvalues—of the graph's adjacency matrix. The spectrum of the graph's adjacency matrix is also called the *spectrum of the graph*.

2. Applying the semicircle law for the spectrum of the uncorrelated random graph

A general form of the semicircle law for real symmetric matrices is the following [20,22,23]. If A is a real symmetric $N\times N$ uncorrelated random matrix, $\langle A_{ij}\rangle\equiv 0$ and $\langle A_{ij}^2\rangle=\sigma^2$ for every $i\neq j$, and with increasing N each moment of each $|A_{ij}|$ remains finite, then in the $N\to\infty$ limit the spectral density—i.e., the density of eigenvalues—of $A/\sqrt{N}$ converges to the semicircular distribution

$$\rho(\lambda)=\begin{cases}(2\pi\sigma^2)^{-1}\sqrt{4\sigma^2-\lambda^2} & \text{if } |\lambda|<2\sigma\\ 0 & \text{otherwise.}\end{cases} \tag{1}$$

This theorem is also known as *Wigner's law* [22], and its extensions to further matrix ensembles have long been used for the stochastic treatment of complex quantum-mechanical systems lying far beyond the reach of exact methods [24,25].

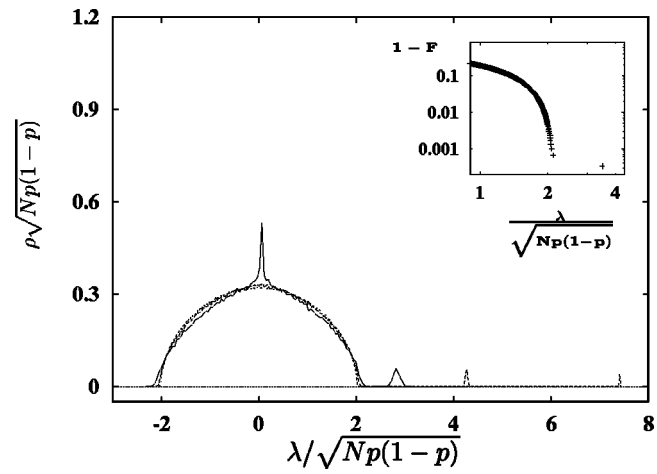

FIG. 1. If $N\to\infty$ and $p=$const, the average spectral density of an uncorrelated random graph converges to a semicircle, the first eigenvalue grows as N, and the second is proportional to $\sqrt{N}$ (see Sec. II A). *Main panel:* The spectral density is shown for $p=0.05$ and three different system sizes: $N=100$ (—), $N=300$ (– –), and $N=1000$ (- - -). In all three cases, the complete spectrum of 1000 graphs was computed and averaged. *Inset:* At the edge of the semicircle, i.e., in the $\lambda\approx\pm 2\sqrt{Np(1-p)}$ regions, the spectral density decays exponentially, and with $N\to\infty$, the decay rate diverges [20,29]. Here, $F(\lambda)=N^{-1}\Sigma_{\lambda_i<\lambda}1$ is the cumulative spectral distribution function, and $1-F$ is shown for a graph with $N=3000$ vertices and 15 000 edges.

Later, the semicircle law was found to have many applications in statistical physics and solid-state physics as well [20,21,26].

Note, that for the adjacency matrix of the uncorrelated random graph many of the semicircle law's conditions do not hold, e.g., the expectation value of the entries is a nonzero constant: $p\neq 0$. Nevertheless, in the $N\to\infty$ limit, the rescaled spectral density of the uncorrelated random graph converges to the semicircle law of Eq. (1) [27]. An illustration of the convergence of the average spectral density to the semicircular distribution can be seen on Fig. 1. It is necessary to make a comment concerning figures here. In order to keep figures simple, for the spectral density plots we have chosen to show the spectral density of the original matrix A and to rescale the horizontal (λ) and vertical (ρ) axes by $\sigma^{-1}N^{-1/2}=[Np(1-p)]^{-1/2}$ and $\sigma N^{1/2}=[Np(1-p)]^{1/2}$.

Some further results on the behavior of the uncorrelated random graph's eigenvalues, relevant for the analysis of real-world graphs as well, include the following: The principal eigenvalue (the largest eigenvalue λ_1) grows much faster than the second eigenvalue: $\lim_{N\to\infty}(\lambda_1/N)=p$ with probability 1, whereas for every $\epsilon>1/2$, $\lim_{N\to\infty}(\lambda_2/N^{\epsilon})=0$ (see Refs. [27,28] and Fig. 1). A similar relation holds for the smallest eigenvalue λ_N: for every $\epsilon>1/2$, $\lim_{N\to\infty}(\lambda_N/N^{\epsilon})=0$. In other words, if $\langle k_i\rangle$ denotes the average number of connections of a vertex in the graph, then λ_1 scales as $pN\approx\langle k_i\rangle$, and the width of the ''bulk'' part of the spectrum, the set of the eigenvalues $\{\lambda_2,\ldots,\lambda_N\}$, scales as $\sigma\sqrt{N}$. Lastly, the semicircular distribution's edges are known to decay

exponentially, and the number of eigenvalues in the $\lambda > O(\sqrt{N})$ tail has been shown to be of the order of 1 [20,29].

B. Real-world graphs

The two main models proposed to describe real-world graphs are the *small-world model* and the *scale-free model*.

1. Small-world graphs

The small-world graph [4,5,30] is created by randomly rewiring some of the edges of a regular [31] ring graph. The regular ring graph is created as follows. First draw the vertices $1,2,\ldots,N$ on a circle in ascending order. Then, for every i, connect vertex i to the vertices lying closest to it on the circle: vertices $i-k/2,\ldots,i-1,i+1,\ldots,i+k/2$, where every number should be understood modulo N (k is an even number). Figure 9 will show later that this algorithm creates a regular graph indeed, because the degree [31] of any vertex is the same number k. Next, starting from vertex 1 and proceeding towards N, perform the *rewiring step*. For vertex 1, consider the first ''forward connection,'' i.e., the connection to vertex 2. With probability p_r, reconnect vertex 1 to another vertex chosen uniformly at random and without allowing multiple edges. Proceed toward the remaining forward connections of vertex 1, and then perform this step for the remaining $N-1$ vertices also. For the rewiring, use equal and independent probabilities. Note that in the small-world model the density of edges is $p=\langle k_i\rangle/(N-1)\approx k/N$. Throughout this paper, we will use only $k>2$.

If we use $p_r=0$ in the small-world model, the original regular graph is preserved, and for $p_r=1$, one obtains a random graph that differs from the uncorrelated random graph only slightly: every vertex has a minimum degree of $k/2$. Next, we will need two definitions. The *separation* between vertices i and j, denoted by L_{ij}, is the number of edges in the shortest path connecting them. The *clustering coefficient* at vertex i, denoted by C_i, is the number of existing edges among the neighbors of vertex i divided by the number of all possible connections between them. In the small-world model, both L_{ij} and C_i are functions of the rewiring probability p_r. Based on the above definitions of $L_{ij}(p_r)$ and $C_i(p_r)$, the characteristics of the small-world phenomenon, which occurs for intermediate values of p_r, can be given as follows [4,5]: (i) the average separation between two vertices, $L(p_r)$, drops dramatically below $L(p_r=0)$, whereas (ii) the average clustering coefficient $C(p_r)$ remains high, close to $C(p_r=0)$. Note that the rewiring procedure is carried out independently for every edge; therefore, the degree sequence and also other distributions in the system, e.g., path length and loop size, decay exponentially.

2. The scale-free model

The scale-free model assumes a random graph to be a *growing* set of vertices and edges, where the location of new edges is determined by a *preferential attachment rule* [10,11]. Starting from an initial set of m_0 isolated vertices, one adds one new vertex and m new edges at every time step t. (Throughout this paper, we will use $m=m_0$.) The m new edges connect the new vertex and m different vertices chosen from the N old vertices. The ith old vertex is chosen with probability $k_i/\Sigma_{j=1,N}k_j$, where k_i is the degree of vertex i. [The density of edges in a scale-free graph is $p=\langle k_i\rangle/(N-1)\approx 2m/N$.] In contrast to the small-world model, the distribution of degrees in a scale-free graph converges to a power law when $N\to\infty$, which has been shown to be a combined effect of growth and the preferential attachment [11]. Thus, in the infinite time or size limit, the scale-free model has no characteristic scale in the degree size [14,32–37].

3. Related models

Lately, numerous other models have been suggested for a *unified description* of real-world graphs [14,32–35,37–40]. Models of growing networks with aging vertices were found to display both heavy tailed and exponentially decaying degree sequences [34–36] as a function of the speed of aging. Generalized preferential attachment rules have helped us better understand the origin of the exponents and correlations emerging in these systems [32,33]. Also, investigations of more complex network models—using aging or an additional fixed cost of edges [12] or preferential growth and random rewiring [37]—have shown, that in the ''frequent rewiring, fast aging, high cost'' limiting case, one obtains a graph with an exponentially decaying degree sequence, whereas in the ''no rewiring, no aging, zero cost'' limiting case the degree sequence will decay as a power law. According to studies of scientific collaboration networks [13,14] and further social and biological structures [12,19,41], a significant proportion of large networks lies between the two extremes. In such cases, the characterization of the system using a small number of algebraic constants could facilitate the classification of real-world networks.

III. TOOLS

A. Analytical

1. The spectrum of the graph

The spectrum of a graph is the set of eigenvalues of the graph's adjacency matrix. The physical meaning of a graph's eigenpair (an eigenvector and its eigenvalue) can be illustrated by the following example. Write each component of a vector $\vec{v}$ on the corresponding vertex of the graph: v_i on vertex i. Next, on every vertex write the sum of the numbers found on the neighbors of vertex i. If the resulting vector is a multiple of $\vec{v}$, then $\vec{v}$ is an eigenvector, and the multiplier is the corresponding eigenvalue of the graph.

The spectral density of a graph is the density of the eigenvalues of its adjacency matrix. For a finite system, this can be written as a sum of δ functions

$$\rho(\lambda):=\frac{1}{N}\sum_{j=1}^{N}\delta(\lambda-\lambda_j), \tag{2}$$

which converges to a continuous function with $N\to\infty$ (λ_j is the jth largest eigenvalue of the graph's adjacency matrix).

The spectral density of a graph can be directly related to the graph's topological features: the kth moment M_k of $\rho(\lambda)$ can be written as

$$M_k=\frac{1}{N}\sum_{j=1}^{N}(\lambda_j)^k=\frac{1}{N}\mathrm{Tr}(A^k)$$
$$=\frac{1}{N}\sum_{i_1,i_2,\cdots,i_k}A_{i_1,i_2}A_{i_2,i_3}\cdots A_{i_k,i_1}. \tag{3}$$

From the topological point of view, $D_k=NM_k$ is the number of directed paths (loops) of the underlying—undirected—graph, that return to their starting vertex after k steps. On a tree, the length of any such path can be an even number only, because these paths contain any edge an even number of times: once such a path has left its starting point by choosing a starting edge, no alternative route for returning to the starting point is available. However, if the graph contains loops of odd length, the path length can be an odd number, as well.

2. Extremal eigenvalues

In an uncorrelated random graph the principal eigenvalue λ_1 shows the density of edges and λ_2 can be related to the conductance of the graph as a network of resistances [42]. An important property of all graphs is the following: the principal eigenvector $\vec{e}_1$ of the adjacency matrix is a non-negative vector (all components are non-negative), and if the graph has no isolated vertices, $\vec{e}_1$ is a positive vector [43]. All other eigenvectors are orthogonal to $\vec{e}_1$, therefore they all have entries with mixed signs.

3. The inverse participation ratios of eigenvectors

The inverse participation ratio of the normalized jth eigenvector $\vec{e}_j$ is defined as [26]

$$I_j=\sum_{k=1}^{N}[(e_j)_k]^4. \tag{4}$$

If the components of an eigenvector are identical, $(e_j)_i=1/\sqrt{N}$ for every i, then $I_j=1/N$. For an eigenvector with one single nonzero component, $(e_j)_i=\delta_{i,i'}$, the inverse participation ratio is 1. The comparison of these two extremal cases illustrates that with the help of the inverse participation ratio, one can tell whether only $O(1)$ or as many as $\mathcal{O}(N)$ components of an eigenvector differ significantly from 0, i.e., whether an eigenvector is localized or nonlocalized.

B. Numerical

1. General real symmetric eigenvalue solver

To compute the eigenpairs of graphs below *the size* $N=5000$, we used the general real symmetric eigenvalue solver of Ref. [44]. This algorithm requires the allocation of memory space to all entries of the matrix, thus to compute the spectrum of a graph of size $N=20\,000$ ($N=1\,000\,000$) using this general method with double precision floating point arithmetic, one would need 3.2 GB (8 TB) memory space and the execution of approximately $30N^2=1.2\times10^{10}$ (3×10^{13}) floating point operations [44]. Consequently, we need to develop more efficient algorithms to investigate the properties of graphs with sizes comparable to real-world networks.

2. Iterative eigenvalue solver based on the thick-restart Lanczos algorithm

The spectrum of a real-world graph is the spectrum of a sparse real symmetric matrix; therefore, the most efficient algorithms that can give a handful of the top n_d eigenvalues—and the corresponding eigenvectors—of a large graph are iterative methods [45]. These methods allow the matrix to be stored in any compact format, as long as matrix-vector multiplication can be carried out at a high speed. *Iterative methods use little memory*: only the nonzero entries of the matrix and a few vectors of size N need to be stored. The price for computational speed lies in the number of the obtained eigenvalues: iterative methods compute only a handful of the largest (or smallest) eigenvalues of a matrix. To compute the eigenvalues of graphs above the size $N=5\,000$, we have developed algorithms using a specially modified version of the thick-restart Lanczos algorithm [46,47]. The modifications and some of the main technical parameters of our software are explained in the following paragraphs.

Even though iterative eigenvalue methods are mostly used to obtain the top eigenvalues of a matrix, after minor modifications the internal eigenvalues in the vicinity of a fixed $\lambda=\lambda_0$ point can be computed as well. For this, extremely sparse matrices are usually ''shift-inverted,'' i.e., to find those eigenvalues of A that are closest to λ_0, the highest and lowest eigenvalues of $(A-\lambda_0 I)^{-1}$ are searched for. However, because of the extremely high cost of matrix inversion in our case, for the computation of internal eigenvalues we suggest using the *''shift-square'' method* with the matrix

$$B=[\lambda^*/2-(A-\lambda_0 I)^2]^{2n+1}. \tag{5}$$

Here λ^* is the largest eigenvalue of $(A-\lambda_0 I)^2$, I is the identity matrix, and n is a positive integer. Transforming the matrix A into B transforms the spectrum of A in the following manner. First, the spectrum is shifted to the left by λ_0. Then, the spectrum is ''folded'' (and squared) at the origin such that all eigenvalues will be negative. Next, the spectrum is linearly rescaled and shifted to the right, with the following effect: (i) the whole spectrum will lie in the symmetric interval $[-\lambda^*/2,\lambda^*/2]$ and (ii) those eigenvalues that were closest to λ_0 in the spectrum of A will be the largest now, i.e., they will be the eigenvalues closest to $\lambda^*/2$. Now, raising all eigenvalues to the $(2n+1)$st power increases the relative difference, $1-\lambda_i/\lambda_j$, between the top eigenvalues λ_i and λ_j by a factor of $2n+1$. This allows the iterative method to find the top eigenvalues of B more quickly. One can compute the corresponding eigenvalues (those being closest to λ_0) of the original matrix, A: if $\vec{b}_1,\vec{b}_2,\ldots,\vec{b}_{n_\mathrm{d}}$ are the normalized eigenvectors of the n_d largest eigenvalues of

B, then for A the n_d eigenvalues closest to λ_0 will be, not necessarily in ascending order, $\vec{b}_1 A \vec{b}_1, \vec{b}_2 A \vec{b}_2, \ldots, \vec{b}_{n_d} A \vec{b}_{n_d}$.

The thick-restart Lanczos method uses memory space for the nonzero entries of the $N \times N$ large adjacency matrix, and n_g+1 vectors of length N, where n_g ($n_g > n_d$) is usually between 10 and 100. Besides the relatively small size of required memory, we could also exploit the fact that the nonzero entries of a graph's adjacency matrix are all 1's: during matrix-vector multiplication—which is usually the most time-consuming step of an iterative method—only additions had to be carried out instead of multiplications.

The numerical spectral density functions of large graphs ($N \geqslant 5000$) of this paper were obtained using the following steps. To compute the spectral density of the adjacency matrix A at an internal $\lambda = \lambda_0$ location, first the n_d eigenvalues closest to λ_0 were searched for. Next, the distance between the smallest and the largest of the obtained eigenvalues was computed. Finally, to obtain $\rho(\lambda_0)$ this distance was multiplied by $N/(n_d-1)$, and was averaged using n_{av} different graphs. We used double precision floating point arithmetic, and the iterations were stopped if (i) at least n_{it} iterations had been carried out and (ii) the lengths of the residual vectors belonging to the n_d selected eigenpairs were all below $\varepsilon = 10^{-12}$ [46].

IV. RESULTS

A. Sparse uncorrelated random graphs: The semicircle law is not universal

In the uncorrelated random graph model of Erdős and Rényi, the total number of edges grows quadratically with the number of vertices: $N_{edge} = N\langle k_i \rangle = Np(N-1) \approx pN^2$. However, in many real-world graphs edges are "expensive," and the growth rate of the number of connections remains well below this rate. For this reason, we also investigated the spectra of such uncorrelated networks, for which the probability of any two vertices being connected changes with the size of the system using $pN^{\alpha} = c = \text{const}$. Two special cases are $\alpha=0$ (the Erdős-Rényi model) and $\alpha=1$. In the second case, $pN \to \text{const}$ as $N \to \infty$, i.e., the average degree remains constant.

For $\alpha < 1$ *and* $N \to \infty$, there exists an infinite cluster of connected vertices (in fact, it exists for every $\alpha \leqslant 1$ [2]). Moreover, the expectation value of any k_i converges to infinity, thus any vertex is almost surely connected to the infinite cluster. The spectral density function converges to the semicircular distribution of Eq. (1) because the total weight of isolated subgraphs decreases exponentially with growing system size. (A detailed analysis of this issue is available in Ref. [48].)

For $\alpha=1$ *and* $N \to \infty$ (see Fig. 2), the probability for a vertex to belong to a cluster of any finite size remains also finite [49]. Therefore, the limiting spectral density contains the weighted sum of the spectral densities of all finite graphs [50]. The most striking deviation from the semicircle law in this case is the elevated central part of the spectral density. The probability for a vertex to belong to an isolated cluster of size s decreases exponentially with s [49]; therefore, the number of large isolated clusters is low. The eigenvalues of a graph with s vertices are bounded by $-\sqrt{s-1}$ and $\sqrt{s-1}$. For these two reasons, the amplitudes of δ functions decay exponentially, as the absolute value of their locations, $|\lambda|$, increases.

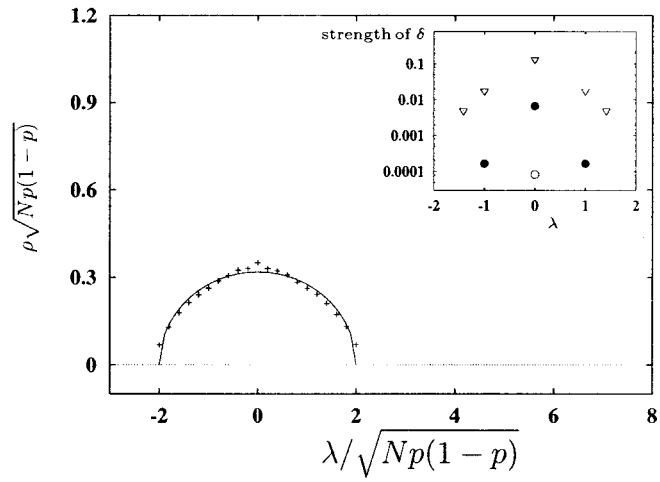

FIG. 2. If $N \to \infty$ and $pN = \text{const}$, the spectral density of the uncorrelated random graph does not converge to a semicircle. *Main panel:* Symbols show the spectrum of an uncorrelated random graph (20 000 vertices and 100 000 edges) measured with the iterative method using $n_{av}=1$, $n_d=101$, and $n_g=250$. A solid line shows the semicircular distribution for comparison. (Note that the principal eigenvalue λ_1 is not shown here because here at any λ_0 point the average first-neighbor distance among $n_d=101$ eigenvalues was used to measure the spectral density.) *Inset:* Strength of δ functions in $\rho(\lambda)$ "caused" by isolated clusters of sizes 1, 2, and 3 in uncorrelated random graphs (see Ref. [50] for a detailed explanation). Symbols are for graphs with 20 000 vertices and 20 000 edges (∇), 50 000 edges (●), and 100 000 edges (○). Results were averaged for three different graphs everywhere.

The principal eigenvalue of this graph converges to a constant: $\lim_{N\to\infty}(\lambda_1) = pN = c$, and $\rho(\lambda)$ will be symmetric in the $N \to \infty$ limit. Therefore, in the limit, all odd moments (M_{2k+1}), and thus the number of all loops with odd length (D_{2k+1}), disappear. This is a salient feature of graphs with tree structure (because on a tree every edge must be used an even number of times in order to return to the initial vertex), indicating that the structure of a sparse uncorrelated random graph becomes more and more treelike. This can also be understood by considering that the typical distance (length of the shortest path) between two vertices on both a sparse uncorrelated random graph and a regular tree with the same number of edges scales as $\ln(N)$. So except for a few shortcuts a sparse uncorrelated random graph looks like a tree.

B. The small-world graph

Triangles are abundant in the graph

For $p_r=0$ the small-world graph is *regular and also periodical*. Because of the highly ordered structure, $\rho(\lambda)$ contains numerous singularities, which are listed in Sec. VI A (see also Fig. 3). Note that $\rho(\lambda)$ has a high third moment. (Remember, that we use only $k>2$.)

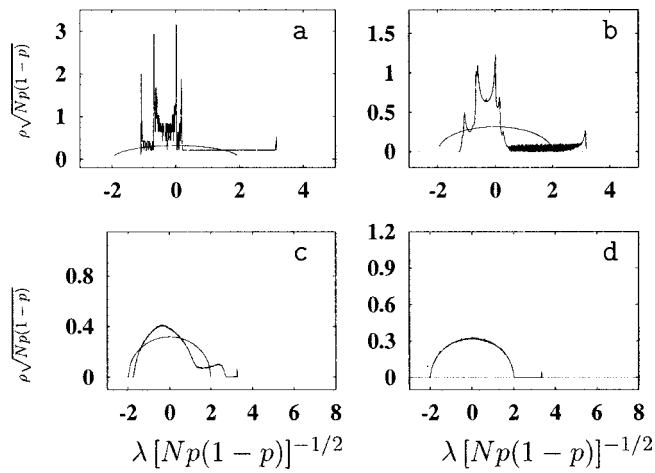

FIG. 3. Spectral densities of small-world graphs using the complete spectra. The solid line shows the semicircular distribution for comparison. (a) Spectral density of the regular ring graph created from the small-world model with $p_r=0$, $k=10$, and $N=1000$. (b) For $p_r=0.01$, the average spectral density of small-world graphs contains sharp maxima, which are the "blurred" remnants of the singularities of the $p_r=0$ case. Topologically, this means that the graph is still almost regular, but it contains a small number of impurities. In other words, after a small perturbation, the system is no longer degenerate. (c) The average spectral density computed for the $p_r=0.3$ case shows that the third moment of $\rho(\lambda)$ is preserved even for very high values of p_r, where there is already no sign of any blurred singularity (i.e., regular structure). This means that even though all remaining regular islands have been destroyed already, *triangles are still dominant.* (d) If $p_r=1$, then the spectral density of the small-world graph converges to a semicircle. In (b), (c), and (d), 1000 different graphs with $N=1000$ and $k=10$ were used for averaging.

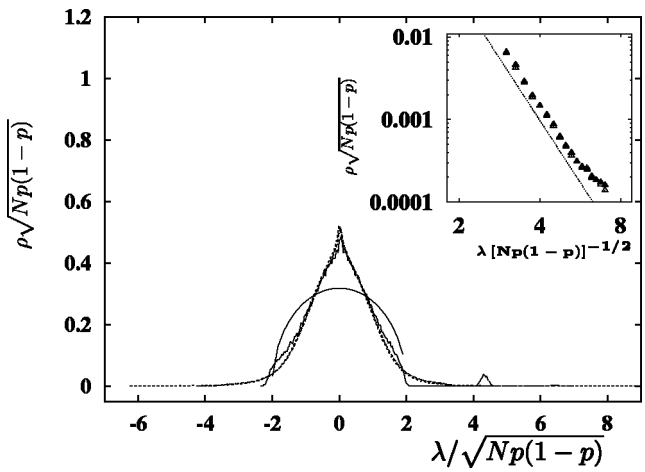

FIG. 4. *Main panel:* The average spectral densities of scale-free graphs with $m=m_0=5$ and $N=100$ (—), $N=1000$ (– –), and $N=7000$ (- - -) vertices. (In all three cases, the complete spectrum of 1000 graphs was used.) Another continuous line shows the semicircular distribution for comparison. Observe that (i) the central part of the scale-free graph's spectral density is trianglelike, not semicircular and (ii) the edges show a power-law decay, whereas the semicircular distribution's edges decay exponentially, i.e., it decays exponentially at the edges [20]. *Inset:* The upper edge of the spectral density for scale-free graphs with $N=40\,000$ vertices, the average degree of a vertex being $\langle k_i\rangle=2m=10$ as before. Note that both axes are logarithmic, indicating that $\rho(\lambda)$ has a power-law tail. Here we used the iterative eigenvalue solver of Sec. III B 2 with $n_d=21$, $n_{av}=3$, and $n_g=60$. The line with the slope -5 in this figure is a guide to the eye.

If we increase p_r such that the small-world region is reached, i.e., the periodical structure of the graph is perturbed, then singularities become blurred and are transformed into high local maxima, but $\rho(\lambda)$ retains a strong skewness (see Fig. 3). This is in good agreement with the results of Refs. [30,51], where it has been shown that the local structure of the small-world graph is ordered; however, already a very small number of shortcuts can drastically change the graph's global structure.

In the $p_r=1$ case the small-world model becomes very similar to the uncorrelated random graph: the only difference is that here, the minimum degree of any vertex is a positive constant $k/2$, whereas in an uncorrelated random graph the degree of a vertex can be any non-negative number. Accordingly, $\rho(\lambda)$ becomes a semicircle for $p_r=1$ (Fig. 3). Nevertheless, it should be noted that as p_r converges to 1, a high value of M_3 is preserved even for p_r close to 1, where all local maxima have already vanished. The third moment of $\rho(\lambda)$ gives the number of triangles in the graph (see Sec. III A 1); the lack of high local maxima, i.e., the remnants of singularities, shows the absence of an ordered structure. From the above we conclude, that—from the spectrum's point of view—the high number of triangles is one of the most basic properties of the small-world model, and it is preserved much longer than regularity or periodicity if the level of randomness p_r is increased. This is in good agreement with the results of Ref. [19] where the high number of small cycles is found to be a fundamental property of small-world networks. As an application, the high number of small cycles results in special diffusion on small-world graphs [61].

C. The scale-free graph

For $m=m_0=1$, the scale-free graph is a tree by definition and its spectrum is symmetric [43]. In the $m>1$ case $\rho(\lambda)$ consists of several well distinguishable parts (see Fig. 4). The "bulk" part of the spectral density—the set of the eigenvalues $\{\lambda_2,\ldots,\lambda_N\}$—converges to a symmetric continuous function which has a trianglelike shape for the normalized λ values up to 1.5 and has power-law tails.

The central part of the spectral density lies well above the semicircle. Since the scale-free graph is fully connected by definition, the increased number of eigenvalues with small magnitudes cannot be accounted to isolated clusters, as before in the case of the sparse uncorrelated random graph. As an explanation, we suggest, that the eigenvectors of these eigenvalues are localized on a small subset of the graph's vertices. (This idea is supported by the high inverse participation ratios of these eigenvectors, see Fig. 7.)

1. The spectral density of the scale-free graph decays as a power law

The inset of Fig. 4 shows the tail of the bulk part of the spectral density for a graph with $N=40\,000$ vertices and

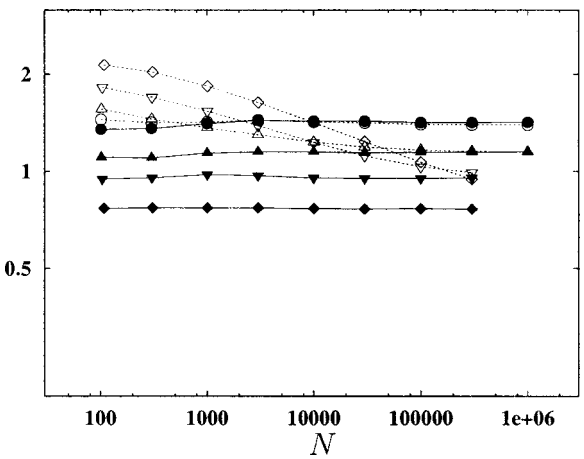

FIG. 5. Comparison of the length of the longest row vector $\sqrt{k_1}$ and the principal eigenvalue λ_1 in scale-free graphs. Open symbols show $\lambda_1/(\sqrt{m}N^{1/4})$, closed symbols show $\sqrt{k_1}/(\sqrt{m}N^{1/4})$. The parameter values are $m=1$ (○), $m=2$ (△), $m=4$ (▽), and $m=8$ (◇). Each data point is an average for nine graphs. For the reader's convenience, data points are connected. If $m>1$ and the network is small, the principal eigenvalue λ_1 of a scale-free graph is determined by the largest row vectors jointly: the largest eigenvalue is above $\sqrt{k_1}$ and the growth rate of λ_1 stays below the maximum possible growth rate, which is $\lambda_1 \propto N^{1/4}$. If $m=1$, or the network is large, the effect of row vectors other than the longest on λ_1 vanishes: the principal eigenvalue converges to the length of the longest row vector, and it grows as $\lambda_1 \propto N^{1/4}$. Our results show a crossover in the growth rate of the scale-free model's principal eigenvalue.

200 000 edges (i.e., $pN=10$). Comparing this to the inset of Fig. 1, where the number of vertices and edges is the same as here, one can observe the *power-law decay* at the edge of the bulk part of $\rho(\lambda)$. As shown later, in Sec. IV D, the power-law decay in this region is caused by localized eigenvectors; these eigenvectors are localized on vertices with the highest degrees. The power-law decay of the degree sequence, i.e., the existence of very high degrees, is, in turn, due to the preferential attachment rule of the scale-free model.

2. The growth rate of the principal eigenvalue shows a crossover in the level of correlations

Since the adjacency matrix of a graph is a non-negative symmetric matrix, the graph's largest eigenvalue λ_1 is also the largest in magnitude (see, e.g., Theorem 0.2 of Ref. [43]). Considering the effect of the adjacency matrix on the base vectors $(b_i)_j=\delta_{ij}$ $(i=1,2,\ldots,N)$, it can be shown that a lower bound for λ_1 is given by the length of the longest row vector of the adjacency matrix, which is the square root of the graph's largest degree k_1. Knowing that the largest degree of a scale-free graph grows as $\sqrt{N}$ [11], one expects λ_1 to grow as $N^{1/4}$ for large enough systems.

Figure 5 shows a rescaled plot of the scale-free graph's largest eigenvalue for different values of m. In this figure, λ_1 is compared to the length of the longest row vector $\sqrt{k_1}$ on the "natural scale" of these values, which is $\sqrt{m}N^{1/4}$ [11]. It is clear that if $m>1$ and the system is small, then through several decades (a) λ_1 is larger than $\sqrt{k_1}$ and (b) the growth rate of λ_1 is well below the expected rate of $N^{1/4}$. In the $m=1$ case, and for large systems, (a) the difference between λ_1 and $\sqrt{k_1}$ vanishes and (b) the growth rate of the principal eigenvalue will be maximal, too. This crossover in the behavior of the scale-free graph's principal eigenvalue is a specific property of sparse growing correlated graphs, and it is a result of the changing level of correlations between the longest row vectors (see Sec. VI B).

3. Comparing the role of the principal eigenvalue in the scale-free graph and the $\alpha=1$ uncorrelated random graph: A comparison of structures

Now we will compare the role of the principal eigenvalue in the $m>1$ scale-free graph and the $\alpha=1$ uncorrelated random graph through its effect on the moments of the spectral density. On Figs. 4 and 5 one can observe that (i) the principal eigenvalue of the scale-free graph is detached from the rest of the spectrum, and (ii) as $N\to\infty$, it grows as $N^{1/4}$ (see also Secs. IV C 2 and VI B). It can be also seen that in the limit, the bulk part will be symmetric, and its width will be constant (Fig. 4 rescales this constant width merely by another constant, namely $[Np(1-p)]^{-1/2}$. Because of the symmetry of the bulk part, in the $N\to\infty$ limit, the third moment of $\rho(\lambda)$ is determined exclusively by the contribution of the principal eigenvalue, which is $N^{-1}(\lambda_1)^3 \propto N^{-1/4}$. For each moment above the third (e.g., for the lth moment), with growing N, the contribution of the bulk part to this moment will scale as $\mathcal{O}(1)$, and the contribution of the principal eigenvalue will scale as $N^{-1+l/4}$. In summary, in the $N\to\infty$ limit, the scale-free graph's first eigenvalue has a significant contribution to the fourth moment; the fifth and all higher moments are determined exclusively by λ_1: the lth moment will scale as $N^{-1+l/4}$.

In contrast to the above, the principal eigenvalue of the $\alpha=1$ uncorrelated random graph converges to the constant $pN=c$ in the $N\to\infty$ limit, and the width of the bulk part also remains constant (see Fig. 2). Given a fixed number l the contribution of the principal eigenvalue to the lth moment of the spectral density will change as $N^{-1}c^l$ in the $N\to\infty$ limit. The contribution of the bulk part will scale as $\mathcal{O}(1)$, therefore all even moments of the spectral density will scale as $\mathcal{O}(1)$ in the $N\to\infty$ limit, and all odd moments will converge to 0.

The difference between the growth rate of the moments of $\rho(\lambda)$ in the above two models (scale-free graph and $\alpha=1$ uncorrelated random graph model) can be interpreted as a sign of different structure (see Sec. III A 1). In the $N\to\infty$ limit, the average degree of a vertex converges to a constant in both models: $\lim_{N\to\infty}\langle k_i\rangle=pN=c=2m$. (Both graphs will have the same number of edges per vertex.) On the other hand, in the limit all moments of the $\alpha=1$ uncorrelated random graph's spectral density converge to a constant, whereas the moments M_l $(l=5,6,\ldots)$ of the scale-free graph's $\rho(\lambda)$ will diverge as $N^{-1+l/4}$. In other words: the number of loops of length l in the $\alpha=1$ uncorrelated random graph will grow as $D_l=NM_l=\mathcal{O}(N)$, whereas for the scale-free graph for every $l\geqslant 3$, the number of these loops will grow as

$D_l = NM_l = \mathcal{O}(N^{l/4})$. From this we conclude that in the limit, the role of loops is negligible in the $\alpha=1$ uncorrelated random graph, whereas it is large in the scale-free graph. In fact, the growth rate of the number of loops in the scale-free graph exceeds all polynomial growth rates: the longer the loop size (l) investigated, the higher the growth rate of the number of these loops ($N^{l/4}$) will be. Note that the relative number of triangles (i.e., the third moment of the spectral density, M_l/N) will disappear in the scale-free graph, if $N \to \infty$.

In summary, the spectrum of the scale-free model converges to a trianglelike shape in the center, and the edges of the bulk part decay slowly. The first eigenvalue is detached from the rest of the spectrum, and it shows an anomalous growth rate. Eigenvalues with large magnitudes belong to eigenvectors localized on vertices with many neighbors. In the present context, the absence of triangles, the high number of loops with length above $l=3$, and the buildup of correlations are the basic properties of the scale-free model.

D. Testing the structure of a "real-world" graph

To analyze the structure of a large sparse random graph (correlated or not), here we suggest several tests that can be performed within $\mathcal{O}(N)$ CPU time, use $\mathcal{O}(N)$ floating point operations, and can clearly differentiate between the three "pure" types of random graph models treated in Sec. IV. Furthermore, these tests allow one to quantify the relation between any real-world graph and the three basic types of random graphs.

1. Extremal eigenvalues

In Sec. III A 2 we have already mentioned that the extremal eigenvalues contain useful information on the structure of the graph. As the spectra of uncorrelated random graphs (Fig. 1) and scale-free networks (Fig. 4) show, the principal eigenvalue of random graphs is often detached from the rest of the spectrum. For these two network types, the remaining bulk part of the spectrum, i.e., the set $\{\lambda_2, \ldots, \lambda_N\}$, converges to a symmetric distribution, thus the quantity

$$R := \frac{\lambda_1 - \lambda_2}{\lambda_2 - \lambda_N} \tag{6}$$

measures the distance of the first eigenvalue from the main part of $\rho(\lambda)$ normalized by the extension of the main part. (R can be connected to the chromatic number of the graph [52].)

Note that in the $N \to \infty$ limit the $\alpha=0$ sparse uncorrelated random graph's principal eigenvalue will scale as $\langle k_i \rangle$, whereas both λ_2 and $|-\lambda_N|$ will scale as $2\sqrt{\langle k_i \rangle}$. Therefore, if $\langle k_i \rangle > 4$, the principal eigenvalue will be detached from the bulk part of the spectrum and R will scale as $(\sqrt{\langle k_i \rangle} - 2)/4$. If, however, $\langle k_i \rangle \leqslant 4$, λ_1 will not be detached from the bulk part, it will converge to 0.

The above explanation and Fig. 6 show that in the $\langle k_i \rangle > 4$ sparse uncorrelated random graph model and the scale-free network, λ_1 and the rest of the spectrum are well separated, which gives similarly high values for R in small systems. In large systems, R of the sparse uncorrelated random graph converges to a constant, while R in the scale-free model decays as a power-law function of N. The reason for this drop is the increasing denominator on the right-hand side of Eq. (6): λ_2 and λ_N are the extremal eigenvalues in the lower and upper long tails of $\rho(\lambda)$, therefore, as N increases, the expectation values of λ_2 and $-\lambda_N$ grow as quickly as that of λ_1. On the other hand, the small-world network shows much lower values of R already for small systems: here, λ_1 is not detached from the rest of the spectrum, which is a consequence of the almost periodical structure of the graph.

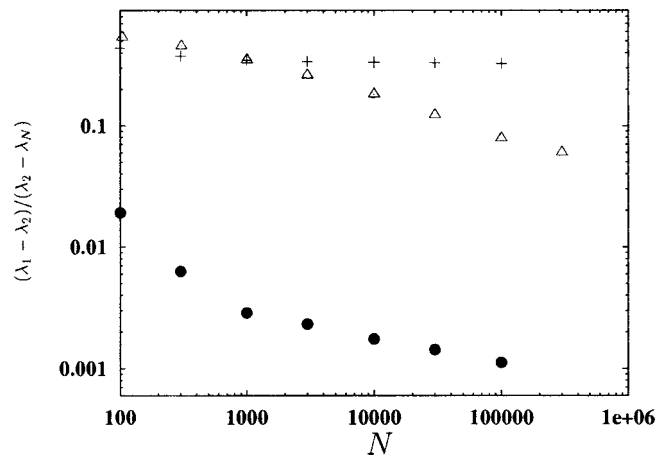

FIG. 6. The ratio $R = (\lambda_1 - \lambda_2)/(\lambda_2 - \lambda_N)$ for sparse uncorrelated random graphs (+), small-world graphs with $p_r = 0.01$ (●), and scale-free networks (△). All graphs have an average degree of $\langle k_i \rangle = 10$, and at each data point, the number of graphs used for averaging was 9. Observe, that for the uncorrelated random graph, R converges to a constant (see Sec. III A 2), whereas it decays rapidly for the two other types of networks, as $N \to \infty$. On the other hand, the latter two network types (small-world and scale-free) differ significantly in their magnitudes of R.

On Fig. 6 graphs with the same number of vertices and edges are compared. For large ($N \geqslant 10\,000$) systems and for sparse uncorrelated random graphs R converges to a constant, whereas for scale-free graphs and small-world networks it decays as a power law. The latter two networks significantly differ in the magnitude of R. In summary, the suggested quantity R has been shown to be appropriate for distinguishing between the following graph structures: (i) periodical or almost periodical (small world), (ii) uncorrelated nonperiodical, and (iii) strongly correlated nonperiodical (scale free).

2. Inverse participation ratios of extremal eigenpairs

Figure 7 shows the inverse participation ratios of the eigenvectors of an uncorrelated random graph, a small-world graph with $p_r = 0.01$, and a scale-free graph. Even though all

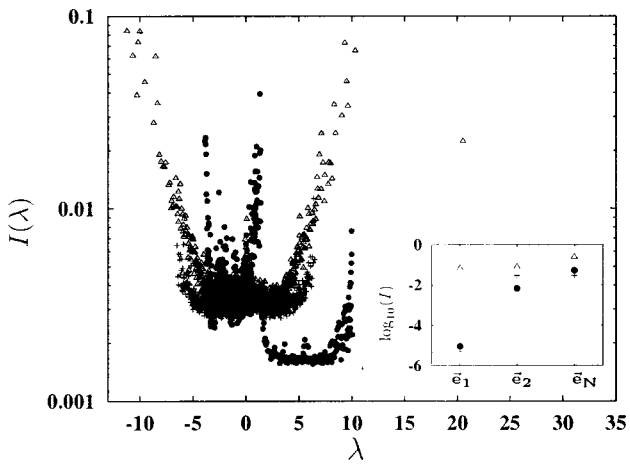

FIG. 7. *Main panel:* Inverse participation ratios of the eigenvectors of three graphs shown as a function of the corresponding eigenvalues: uncorrelated random graph (+), small-world graph with $p_r = 0.01$ (●), and scale-free graph (△). All three graphs have $N = 1000$ vertices, and the average degree of a vertex is $\langle k_i \rangle = 10$. Observe that the eigenvectors of the sparse uncorrelated random graph and the small-world network are usually nonlocalized [$I(\lambda)$ is close to $1/N$]. On the contrary, eigenvectors belonging to the scale-free graph's extremal eigenvalues are highly localized with $I(\lambda)$ approaching 0.1. Note also that for $\lambda \approx 0$, the scale-free graph's $I(\lambda)$ has a significant "spike" indicating again the localization of eigenvectors. *Inset:* Inverse participation ratios of the first, second, and Nth eigenvectors of an uncorrelated random graph (+), a small-world graph with $p_r = 0.01$ (●), and a scale-free graph (△). For each data point, the number of vertices was $N = 300\,000$ and the number of edges was 1 500 000. Clearly, the principal eigenvector of the scale-free graph is localized, while the principal eigenvector of the other two systems (the uncorrelated models) is not. Note also that the inverse participation ratios of the second and Nth eigenvectors clearly differ in the small-world graph—the spectrum of this graph has already been shown to be strongly asymmetric—whereas in the uncorrelated random graph the inverse participation ratios of $\vec{e}_2$ and $\vec{e}_N$ are approximately the same. Thus, with the help of the inverse participation ratios of $\vec{e}_1$, $\vec{e}_2$, and $\vec{e}_N$, one can identify the three main types of random graphs used here.

three graphs have the same number of vertices ($N = 1000$) and edges (5000), one can observe rather specific features (see also the inset of Fig. 7).

The uncorrelated random graph's eigenvectors show very little difference in their level of localization, except for the principal eigenvector, which is much less localized than the other eigenvectors; $I(\lambda_2)$ and $I(\lambda_N)$ are almost equal. For the small-world graph's eigenvectors, $I(\lambda)$ has many different plateaus and spikes; the principal eigenvector is not localized, and the second and Nth eigenvectors have high, but different, $I(\lambda)$ values. The eigenvectors belonging to the scale-free graph's largest and smallest eigenvalues are localized on the "largest" vertices. The long tails of the bulk part of $\rho(\lambda)$ are due to these vertices. All three investigated eigenvectors ($\vec{e}_1$, $\vec{e}_2$, and $\vec{e}_N$) of the scale-free graph are highly localized. Consequently, the inverse participation ratios of the eigenvectors $\vec{e}_1$, $\vec{e}_2$, and $\vec{e}_N$ are handy for the identification of the three basic types of random graph models used.

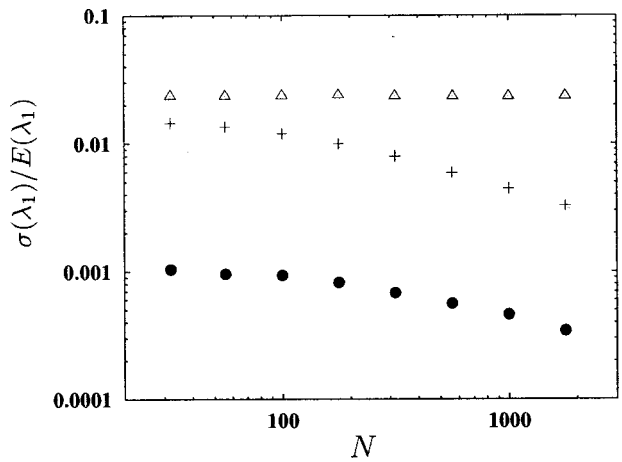

FIG. 8. Size dependence of the relative variance of the principal eigenvalue, i.e., $\sigma(\lambda_1)/E(\lambda_1)$, for sparse uncorrelated random graphs (+), small-world graphs with $p_r = 0.01$ (●), and scale-free graphs (△). The average degree of a vertex is $\langle k_i \rangle = 10$, and 1000 graphs were used for averaging at every point. Observe that in the uncorrelated random graph and the small-world model $\sigma(\lambda_1)/E(\lambda_1)$ decays with increasing system size; however, for scale-free graphs with the same number of edges and vertices, it remains constant.

E. Structural variances

Relative variance of the principal eigenvalue for different types of networks: The scale-free graph and self-similarity

Figure 8 shows the relative variance of the principal eigenvalue, i.e., $\sigma(\lambda_1)/E(\lambda_1)$, for the three basic random graph types.

For nonsparse uncorrelated random graphs ($N \to \infty$ and $p = \text{const}$) this quantity is known to decay at a rate which is faster than exponential [28,53]. Comparing sparse graphs with the same number of vertices and edges, one can see that in the sparse uncorrelated random graph and the small-world model the relative variance of the principal eigenvalue drops quickly with growing system size. In the scale-free model, however, the relative variance of the principal eigenvalue's distribution remains constant with an increasing number of vertices.

In fractals, fluctuations do not disappear as the size of the system is increased, while in the scale-free graph, the relative variance of the principal eigenvalue is independent of system size. In this sense, the scale-free graph resembles self-similar systems.

V. CONCLUSIONS

We have performed a detailed analysis of the complete spectra, eigenvalues, and the eigenvectors' inverse participation ratios in three types of sparse random graphs: the sparse uncorrelated random graph, the small-world model, and the scale-free network. Connecting the topological features of these graphs to algebraic quantities, we have demonstrated that (i) the semi circle law is not universal, not even for the uncorrelated random graph model; (ii) the small-world graph is inherently noncorrelated and contains a high number of

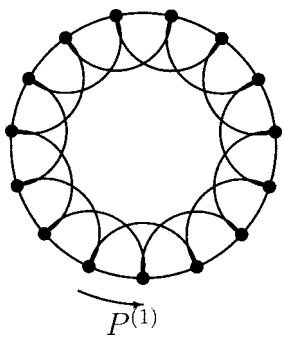

FIG. 9. The regular ring graph obtained from the small-world model in the $p_r=0$ case: rotations ($P^{(n)}$ for every $n=0,1,\ldots,N-1$) are symmetry operations of the graph. The $P^{(n)}$ operators (there are N of them) can be used to create a full orthogonal basis of the adjacency matrix A: taking any $P^{(n)}$, it commutes with A, therefore they have a common full orthogonal system of eigenvectors. (For a clear illustration of symmetries, this figure shows a graph with only $N=15$ vertices and $k=4$ connections per vertex.)

triangles; (iii) the spectral density of the scale-free graph is made up of three, well distinguishable parts (center, tails of bulk, first eigenvalue), and as $N\to\infty$, triangles become negligible and the level of correlations changes.

We have presented practical tools for the identification of the above-mentioned basic types of random graphs and further, for the classification of real-world graphs. The robust eigenvector techniques and observations outlined in this paper combined with previous studies are likely to improve our understanding of large sparse correlated random structures. Examples for algebraic techniques already in use for large sparse correlated random structures are analyses of the Internet [6,18] and search engines [54,62] and mappings [55,56] of the World-Wide Web. Besides the improvement of these techniques, the present work may turn out to be useful for analyzing the correlation structure of the transactions between a very high number of economical and financial units, which has already been started in, e.g., Refs. [57–59]. Lastly, we hope to have provided quantitative tools for the classification of further "real-world" networks, e.g., social and biological networks.

Note added in proof. Recently, we were made aware of a manuscript by Goh, Kahng, and Kim [63] investigating the spectral properties of scale-free networks. Also, our attention has been drawn to a recent publication of Bauer and Golinelli [64] on the spectral properties of uncorrelated random graphs.

ACKNOWLEDGMENTS

We thank D. Petz, G. Stoyan, G. Tusnády, K. Wu, and B. Kahng for helpful discussions and suggestions. This research was partially supported by a HNSF Grant No. OTKA T033104 and NSF Grant No. PHY-9988674.

APPENDIX A: THE SPECTRUM OF A SMALL-WORLD GRAPH FOR $p_r=0$ REWIRING PROBABILITY

1. Derivation of the spectral density

If the rewiring probability of a small-world graph is $p_r=0$, then the graph is regular, each vertex is connected to its k nearest neighbors, and the eigenvalues can be computed using the graph's symmetry operations. Rotational symmetry operations can be easily recognized, if the vertices of the graph are drawn along the perimeter of a circle (see Fig. 9): let $P^{(n)}$ ($n=0,1,\ldots,N-1$) denote the symmetry operation that rotates the graph by n vertices in the anticlockwise direction. Being a symmetry operation, each $P^{(n)}$ commutes with the adjacency matrix A, and they have a common full orthogonal system of eigenvectors.

Now, we will create a full orthogonal basis of A. (We will treat only the case when N is an even number; odd N's can be treated similarly.) It is known that the eigenvalues of A are real; however, to simplify calculations, we will use complex numbers first. The eigenvectors of every $P^{(n)}$ are $\vec{e}_1,\vec{e}_2,\ldots,\vec{e}_N$,

$$(e_l)_j=\exp\left(2\pi i\frac{jl}{N}\right), \tag{A1}$$

where $l=0,2,\ldots,N-1$ and $i=\sqrt{-1}$. The eigenvalue of $P^{(n)}$ on $\vec{e}_l$ is

$$s_l^{(n)}=\exp\left(2\pi i\frac{nl}{N}\right). \tag{A2}$$

By adding these values pairwise, one can obtain the N eigenvalues of the graph

$$\lambda_l=2\sum_{j=1}^{k/2}\cos\left(2\pi\frac{jl}{N}\right). \tag{A3}$$

In the previous exponential form the right-hand side is a summation for a geometrical series; therefore,

$$\lambda_l=\frac{\sin[(k+1)l\pi/N]}{\sin(l\pi/N)}-1. \tag{A4}$$

In the $N\to\infty$ limit, this converges to

$$\lambda(x)=\frac{\sin[(k+1)x]}{\sin(x)}-1, \tag{A5}$$

where x is evenly distributed in the interval $[0,\pi]$.

2. Singularities of the spectral density

The spectral density is singular in $\lambda=\lambda(x)$, if and only if $(d\lambda/dx)(x)=0$, which is equivalent to

$$(k+1)\tan(x)=\tan[(k+1)x]. \tag{A6}$$

Since k is an even number, both this equation and Eq. (A5) are invariant under the transformation $x\mapsto\pi-x$, therefore only the $x\epsilon[0,\pi/2]$ solutions will give different λ values. If $k=10$ (see Fig. 3), Eq. (A6) has $k/2+1=6$ solutions in $[0,\pi/2]$, which are $x=0$, 0.410, 0.704, 0.994, 1.28, and $\pi/2$. Therefore, according to Eq. (A5), in the $N\to\infty$ limit the spectral density will be singular in the following points:

$$\lambda_i=-3.46,-2.19,-2,0.043,0.536,\ \text{and}\ k=10. \tag{A7}$$

APPENDIX B: CROSSOVER IN THE GROWTH RATE OF THE SCALE-FREE GRAPH'S PRINCIPAL EIGENVALUE

The largest eigenvalue is influenced only by the longest row vector if and only if the two longest row vectors are almost orthogonal:

$$\vec{v}_1\vec{v}_2 \ll |\vec{v}_1||\vec{v}_2|. \tag{B1}$$

For $m>1$, the left-hand side (lhs) of Eq. (B1) is the number of simultaneous 1's in the two longest row vectors, and the rhs can be approximated with $|\vec{v}_1|^2=k_1$, the largest degree of the graph. It is known [11] that for large j $(j>i)$, the jth vertex will be connected to vertex i with probability $P_{ij}=m/(2\sqrt{ij})$. Thus, we can write Eq. (B1) in the following forms:

$$\sum_{t=1}^{N} P_{1t}^2 \ll \sum_{t=1}^{N} P_{1t} \tag{B2}$$

or

$$\frac{\sqrt{N_c}}{\ln N_c} \gg \frac{m}{4}, \tag{B3}$$

where N_c is the critical system size.

[1] P. Erdős and A. Rényi, Publ Math **6**, 290 (1959); Publ. Math. Inst. Hung. Acad. Sci. **5**, 17 (1960); **5**, 290 (1959); Acta Math. Acad. Sci. Hung. **12**, 261 (1961).
[2] B. Bollobás, *Random Graphs* (Academic, London, 1985).
[3] S. Redner, Eur. Phys. J. B **4**, 131 (1998).
[4] D.J. Watts and S.H. Strogatz, Nature (London) **393**, 440 (1998).
[5] D.J. Watts, *Small Worlds: The Dynamics of Networks Between Order and Randomness (Princeton Reviews in Complexity)* (Princeton University Press, Princeton, NJ, 1999).
[6] M. Faloutsos, P. Faloutsos, and C. Faloutsos, Comput. Commun. Rev. **29**, 251 (1999).
[7] L.A. Adamic and B.A. Huberman, Nature (London) **401**, 131 (1999).
[8] R. Albert, H. Jeong, and A.-L. Barabási, Nature (London) **401**, 130 (1999).
[9] H. Jeong, B. Tombor, R. Albert, Z.N. Oltvai, and A.-L. Barabási, Nature (London) **407**, 651 (2000).
[10] A.-L. Barabási and R. Albert, Science **286**, 509 (1999).
[11] A.-L. Barabási, R. Albert, and H. Jeong, Physica A **272**, 173 (1999).
[12] L.A.N. Amaral, A. Scala, M. Barthélémy, and H.E. Stanley, e-print cond-mat/0001458.
[13] A.L. Barabási, H. Jeong, E. Ravasz, Z. Néda, T. Vicsek, and A. Schubert (unpublished).
[14] M.E.J. Newman, Proc. Natl. Acad. Sci. USA **98**, 404 (2001);e-print cond-mat/0011144.
[15] A. Medina, I. Matta, and J. Byers, Comput Commun. Rev. **30**, 18 (2000).
[16] R. Cohen, K. Erez, D. ben-Avraham and S. Havlin, Phys. Rev. Lett. **85**, 4626 (2000).
[17] R. Cohen, K. Erez, D. ben-Avraham, and S. Havlin, Phys. Rev. Lett. **86**, 3682 (2001).
[18] A. Broder, R. Kumar, F. Maghoul, P. Raghavan, S. Rajalopagan, R. Stata, A. Tomkins, and J. Wiener, in Proceeding of the 9th International World-Wide Web Conference, 2000 (un published), see (http://www.almaden.ibm.com/cs/k53/www9.final/).
[19] Petra M. Gleiss, Peter F. Stadler, Andreas Wagner, and David A. Fell (unpublished).
[20] M.L. Mehta, *Random Matrices*, 2nd ed. (Academic, New York, 1991).
[21] A. Crisanti, G. Paladin, and A. Vulpiani, *Products of Random Matrices in Statistical Physics*, Springer Series in Solid-State Sciences Vol. 104 (Springer, Berlin, 1993).
[22] E.P. Wigner, Ann. Math. **62**, 548 (1955); **65**, 203 (1957); **67**, 325 (1958).
[23] F. Hiai and D. Petz *The Semicircle Law, Free Random Variables and Entropy* (American Mathematical Society, Providence, 2000), Section 4.1.
[24] F.J. Dyson, J. Math. Phys. **3**, 140 (1962).
[25] E.P. Wigner, SIAM Rev. **9**, 1 (1967).
[26] T. Guhr, A. Müller-Groeling, and H.A. Weidenműller, Phys. Rep. **299**, 189 (1998).
[27] F. Juhász, in *Algebraic Methods in Graph Theory* (North Holland, Amsterdam, 1981), pp. 313–316.
[28] D. Cvetkovic and P. Rowlinson, Linear Multilinear Algebra **28**, 3 (1990).
[29] B.V. Bronx, J. Math. Phys. **5**, 215 (1964).
[30] M.E.J. Newman, C. Moore, and D.J. Watts, Phys. Rev. Lett. **84**, 3201 (2000).
[31] The number of edges meeting at one vertex of a graph is called the degree of that vertex, and a graph is called regular if every vertex has the same degree.
[32] P.L. Krapivsky and S. Redner, e-print cond-mat/0011094.
[33] P.L. Krapivsky, G.J. Rodgers, and S. Redner, e-print cond-mat/0012181.
[34] S.N. Dorogovtsev and J.F.F. Mendes, Phys. Rev. E **62**, 1842 (2000).
[35] S.N. Dorogovtsev, J.F.F. Mendes, and A.N. Samukhin, e-print cond-mat/0011077.
[36] S.N. Dorogovtsev and J.F.F. Mendes, Phys. Rev. E **63**, 056125 (2001).
[37] R. Albert and A.-L. Barabási, Phys. Rev. Lett. **85**, 5234 (2000).
[38] G. Bianconi and A.-L. Barabási, e-print cond-mat/0011224.
[39] G. Bianconi, and A.-L. Barabási, e-print cond-mat/0011029.
[40] A. Vazquez, e-print cond-mat/0006132.
[41] J.M. Montoya and R.V. Solé (unpublished); R.V. Solé and J. M. Montoya (unpublished).
[42] *Handbook of Combinatorics*, edited by R.L. Graham, M. Grötschel, and L. Lovász (North-Holland, Amsterdam, 1995).
[43] D. M. Cvetković, M. Doob, and H. Sachs, *Spectra of Graphs* (VEB Deutscher Verlag der Wissenschaften, Berlin, 1980).
[44] W.H. Press, S.A. Teukolsky, W.T. Vetterling, and B.P. Flan-

nery, *Numerical Recipes in C*, 2nd ed. (Cambridge University Press, Cambridge, 1995), Secs. 11.2 and 11.3.

[45] B.N. Parlett, *The Symmetric Eigenvalue Problem* (SIAM, Philadelphia, PA, 1998).

[46] K. Wu, A. Canning, H.D. Simon, and L.-W. Wang, J. Comput. Phys. **154**, 156 (1999).

[47] K. Wu and H. Simon, Lawrence Berkeley National Laboratory Report No. 41412, 1998.

[48] B. Bollobás and A.G. Thomason, Random Graphs '83 (Poznan, Poland, 1983).

[49] If $n_{s,e}$ denotes the number of isolated clusters with s vertices and e edges, then the number of isolated clusters of size s can be written as $n_s=\Sigma_{e=s-1}^{s(s-1)/2} n_{s,e}$. The $e=s-1$ case corresponds to stars of size s, and $n_{s,s-1}$ can be given as $\binom{N}{s} s p^{s-1}(1-p)^{s(N-s)+[s(s-1)/2]-(s-1)}$. If $N\to\infty$ and $pN\to c$, then for any finite s this converges to $Nf(s)$, where $f(s)=(2\pi)^{-1/2}s^{-s+1/2}c^{s-1}\exp(s-sc)$, which is an exponentially decreasing function of s, if $c>1$. Similarly to this case, in the $N\to\infty$ and $pN\to c$ limit, for all values of e, $n_{s,e}$ is an exponentially decaying function of s, if $c>1$. Since the number of possible e values for a fixed s is a polynomial function of s, n_s will also decay exponentially, if $c>1$, $N\to\infty$ and $pN\to c$.

[50] In a graph with N vertices, the contribution of one isolated vertex to the spectral density is $N^{-1}\delta(\lambda)$, and the contribution of an isolated cluster with two vertices is $N^{-1}[\delta(\lambda+1)+\delta(\lambda-1)]$. An isolated cluster with three vertices and two edges will give $N^{-1}[\delta(\lambda+\sqrt{2})+\delta(\lambda)+\delta(\lambda-\sqrt{2})]$, and one with three vertices and three edges adds $N^{-1}[2\delta(\lambda+1)+\delta(\lambda-2)]$ to the spectral density.

[51] M. Barthélémy and L.A.N. Amaral, Phys. Rev. Lett. **82**, 3180 (1999); **82**, 5180(E) (1999).

[52] A graph is said to be properly colored if any two vertices connected by an edge have different colors, and the *chromatic number* $\chi(G)$ of a graph G is the smallest such natural number k for which the graph can be properly colored using k colors. On a complete graph (a graph where any two vertices are connected) with N vertices, $\chi=N$, while on a tree, $\chi=2$. It should be noted that, in general, the chromatic number of a graph is not determined by its spectrum; in fact, there exist graphs with identical spectra and different chromatic numbers [43]. A well-known relation [60] connecting the *chromatic number and the extremal eigenvalues* of any graph is the following: $\chi(G)\geqslant 1+\lambda_1/(-\lambda_N)$. If the bulk part of the spectrum is symmetrical and the first eigenvalue is separated—as is the case for uncorrelated random graphs and scale-free networks—then R can be written as $[1+\lambda_1/(-\lambda_N)]/z-1\leqslant\chi/z-1$.

[53] C. McDiarmid, *Surveys in Combinatorics, 1989 (Norwich, 1989)*, London Math. Soc. Lecture Note Series Vol. 141 (Cambridge University Press, Cambridge, 1989), pp. 148–188.

[54] J. Kleinberg, S.R. Kumar, P. Raghavan, S. Rajagopalan, and A. Tomkins, Proceedings of the International Conference on Combinations and Computers, 1999 (unpublished); see also the homepage of the "CLEVER" project at ⟨http://www.almaden.ibm.com/cs/k53/clever.html⟩.

[55] The CAIDA Plankton project: Visualizing NLANR's Web Cache Hierarchy ⟨http://www.caida.org/tools/visualization/plankton/⟩.

[56] Y. Shavitt, X. Sun, A. Wool, and B. Yener, Lucent Technologies Technical Report No. 10009674-000214-01TM, 2000.

[57] L. Laloux, P. Cizeau, J.-P. Bouchaud, and M. Potters, Phys. Rev. Lett. **83**, 1467 (1999).

[58] V. Plerou, P. Gopikrishnan, B. Rosenow, L.A.N. Amaral, and H.E. Stanley, Phys. Rev. Lett. **83**, 1471 (1999).

[59] R.N. Mantegna, e-print cond-mat/9802256.

[60] N. Biggs, *Algebraic Graph Theory* (Cambridge University Press, Cambridge, 1974).

[61] S. Jespersen, I.M. Sokolov, and A. Blumen, Phys. Rev. E **62**, 4405 (2000).

[62] The "citation graph analysis" feature of the NECI Scientific Literature Digital Library [formerly CiteSeer (http://citeseer.nj.nec.com/)] is based on algebraic search techniques from Ref. [54].

[63] K.-I. Goh, B. Kahng, and D. Kim, e-print cond-mat/0103337.

[64] M. Bauer and O. Golinelli, J. Stat. Phys. **103**, 301 (2001).